Research in Astronomy and Astrophysics, 25:015001 (19pp), 2025 January
https://doi.org/10.1088/1674-4527/ad89a8
CSTR:32081.14.RAA.ad89a8

Statistical Research on Megahertz-peaked Spectra Pulsars

Hong-Bing Cai[1], Li Chen[2], Shi-Dang Li[2], Kai Wang[2], and Hang Liu[2]
[1] JSNU SPBPU Institute of Engineering & SINO RUSSIAN Institute, Jiangsu Normal University, Xuzhou 221116, China; hbcai@jsnu.edu.cn
[2] School of Physics and Electronic Engineering, Jiangsu Normal University, Xuzhou 221116, China
Received 2024 June 26; revised 2024 September 27; accepted 2024 October 15; published 2025 January 2

Abstract

Megahertz-peaked spectra (MPS) pulsars are referred as cases whose radio spectra turn over around 100 MHz. We identified 53 MPS pulsars based on the spectral data from the literature, and statistically analyzed the spatial location distribution, the magnetic field-period distribution, peak frequencies, spectral indices, and dispersion measures of these MPS pulsars. We found that there is a strong positive correlation between the dispersion measures and the peak frequencies of MPS pulsars, and negative correlations of the dispersion measures with spectral indices and the ages are also found. Such correlations suggest that the interstellar medium is an important factor that affects observational properties of MPS pulsars.

Key words: (stars:) pulsars: general – radio continuum: general – ISM: general

1. Introduction

Radio spectra of pulsars can provide the important information on the pulsars' radiation mechanism. Sieber (1973) studied the radio spectra of 27 pulsars and found that the radio spectra of most pulsars can be described by a simple power-law spectrum: $S_\nu = S_0 \nu^\alpha$, where S_ν is the flux density of the pulsar at frequency ν, S_0 is the flux density at 1 GHz, and α is the spectral index, which is generally negative. Sieber (1973) also found a class of pulsars with an inverted spectral shape, and these pulsars' spectral peaks are near several hundred megahertz. In this paper, we refer to such low-frequency inverted spectra pulsars as megahertz-peaked spectra (MPS) pulsars.

In order to investigate the physical mechanisms behind MPS pulsars, Sieber (1973) tried to fit the low-frequency inversion by the synchrotron self-absorption (SSA) model and the free–free absorption (FFA) model. According to Kellermann (1966), if the brightness temperature of synchrotron radiation by the electrons in magnetic field approaches the kinetic temperature of electrons, the electrons' self-absorption is not negligible, which is so-called SSA. For pulsars, the SSA processes occur within the magnetosphere of pulsars. FFA is mainly due to the cold electrons between the emitting source and the observer absorbing the emission passing through them, so the FFA processes often occur outside the pulsars, i.e., the interstellar medium is the main location for FFA. Marcote et al. (2015) used the SSA, FFA, and SSA plus Razin effect models to fit the low-frequency inversion spectrum of LS 5039, and it seems that SSA plus the Razin effect can match better than SSA or FFA. Jankowski et al. (2018) identified 10 pulsars with the inverted phenomena in the frequency range from 50 to 100 MHz. They also speculated that the reason for the inverted spectra is the FFA process occurring in the interstellar medium around the pulsar. Cong et al. (2021) constructed maps of FFA using a cylindrical emissivity model and the NE2001 free electron distribution model. According to their maps, the interstellar medium undergoes FFA more drastically in the low-frequency band.

Research also has been conducted on whether there are low-frequency inversion phenomena in millisecond pulsars. Kuzmin & Losovsky (2001) studied the radiation spectra of 30 millisecond pulsars in the band 102–111 MHz. They found that most millisecond pulsars did not exhibit low-frequency inversion behavior, and only PSR J1012+5307 possibly has an inverted spectrum near 100 MHz. They also pointed out that the absence of low-frequency inversion in most millisecond pulsars may be related to the fact that the structures of their radiation regions are different from those of normal pulsars. According to Kuzmin & Losovsky (2001), millisecond pulsars have a smaller light cylinder, which may alter the magnetic field configuration from a pure dipole to multipole. The small divergence in multipole can suppress the appearance of low-frequency turn over. In fact, the magnetic configuration of millisecond pulsars after accretion is complex, and a local strong magnetic zone may exist on account of the accretion induced magnetic redistribution (e.g., Zhang & Kojima 2006). In recent years, more research has been conducted on the low-frequency inversion phenomena of millisecond pulsars (e.g., and Kuniyoshi et al. 2015; Wang et al. 2021; Lee et al. 2022). In particular, Wang et al. (2021) found a millisecond pulsar, J0318+0253, with the weakest radio flux ever recorded, and its peak inversion frequency may be near 350 MHz. They suggested that the inversion phenomena of millisecond pulsars may be related to the intrinsic properties of millisecond pulsars themselves.

Table 1
Pulsars Previously Thought to have Inversion Spectra

Pulsar	DM/pc cm^{-3}	T_c/kyr	α_0	$\nu^0_{\rm peak}$/ GHz	P/s	$P1$	B/G	References
J0034-0721	11	36600	−3	0.055	0.94295	4.08E-16	6.28E+11	Lee et al. (2022)
J0141+6009	34.9	49500	−1.6	0.1	1.22295	3.91E-16	7.00E+11	Malofeev et al. (1994)
J0304+1932	15.7	17000	−1.58	0.102	1.38758	1.30E-15	1.36E+12	Izvekova et al. (1981)
J0323+3944	26	75600	−2.5	0.06	3.03207	6.36E-16	1.4E+12	Malofeev et al. (1994)
J0332+5434	27	5530	−3.8	0.27	0.71452	2.05E-15	1.22E+12	Malofeev et al. (1994)
J0358+5413	57	564	−1.3	0.1	0.15638	4.39E-15	8.39E+11	Malofeev et al. (1994)
J0437-4715*	2.6	1590000	−2.4	0.285	0.00575	5.73E-20	5.81E+8	Lee et al. (2022)
J0452-1759	40	1510	−2.6	0.1	0.54894	5.75E-15	1.8E+12	Malofeev et al. (1994)
J0528+2200	51	1480	−3.2	0.08	3.74554	4.01E-14	1.24E+12	Malofeev et al. (1994)
J0543+2329	77.7	253	−1.2	0.2	0.24597	1.54E-14	1.97E+12	Malofeev et al. (1994)
J0614+2229	97	89	−3.8	0.08	0.33496	5.94E-14	4.52E+12	Malofeev et al. (1994)
J0630-2834	34	2770	−2.5	0.098	1.24442	7.12E-15	3.01E+12	Lee et al. (2022)
J0659+1414	13.9	111	−2.37	0.15	0.38493	5.49E-14	4.65E+12	Izvekova et al. (1981)
J0742-2822	74	157	−1.8	0.25	0.16676	1.68E-14	1.69E+12	Malofeev et al. (1994)
J0809-4753	228.3	2820	−2.37	0.123	0.54720	3.08E-15	1.31E+12	Jankowski et al. (2018).
J0814+7429	5.8	122000	−1.7	0.05	1.29224	1.68E-16	4.72E+11	Malofeev et al. (1994)
J0820-1350	41	9320	−2.3	0.15	1.23813	2.11E-15	1.63E+12	Malofeev et al. (1994)
J0826+2637	19.5	4920	−1.8	0.06	0.53066	1.71E-15	9.64E+11	Malofeev et al. (1994)
J0835-4510	67.8	11.3	−3.58	0.38	0.08933	1.25E-13	3.38E+12	Izvekova et al. (1981)
J0837+0610	13	2970	−3.4	0.053	1.27377	6.80E-15	2.98E+12	Jankowski et al. (2018).
J0922+0638	27	497	−1.62	0.041	0.43063	1.37E-14	2.46E+12	Jankowski et al. (2018).
J0934-5249	100	4920	−3.6	0.36	1.44478	4.65E-15	2.62E+12	Jankowski et al. (2018).
J0942-5657	159.7	323	−2.7	0.10	0.80816	3.96E-14	5.73E+12	Jankowski et al. (2018).
J0943+1631	20.3	189000	−1.6	0.059	1.08742	9.11E-17	3.18E+11	Jankowski et al. (2018).
J0953+0755	3	17500	−2.6	0.104	0.25307	2.30E-16	2.44E+11	Lee et al. (2022)
J1001-5507	130.3	441	−1.75	0.19	1.43663	5.16E-14	8.71E+12	Jankowski et al. (2018)
J1012+5307*	9	4860000	−1.7	0.1	0.00526	1.71E-20	3.04E+08	Kuzmin & B. Y. Losovsky (2001)
J1057-5226	30	535	−2.04	0.05	0.19711	5.84E-15	1.09E+12	Jankowski et al. (2018)
J1136+1551	4.8	5040	−2.0	0.03	1.18791	3.73E-15	2.13E+12	Malofeev et al. (1994)
J1239+2453	9	22800	−2.2	0.04	1.38245	9.60E-16	1.17E+12	Malofeev et al. (1994)
J1453-6413	71	1040	−2.5	0.14	0.17949	2.74E-15	7.1E+11	Lee et al. (2022)
J1456-6843	8.6	42200	−2.6	0.15	0.26338	9.90E-17	1.63E+11	Malofeev et al. (1994)
J1509+5531	19.6	2340	−1.9	0.08	0.73968	5.00E-15	1.95E+12	Malofeev et al. (1994)
J1543+0929	35.0	27400	−1.2	0.08	0.74844	4.32E-16	5.76E+11	Sieber (1973)
J1607-0032	10.7	21800	−1.5	0.09	0.42182	3.06E-16	3.64E+11	Malofeev et al. (1994)
J1614+0737	21	8100	−3.8	0.1	1.20680	2.36E-15	1.71E+12	Malofeev et al. (1994)
J1645-0317	36	3450	−2.4	0.08	0.38769	1.78E-15	8.41E+11	Malofeev et al. (1994)
J1651-4246	482	2820	−2.19	0.09	0.84408	4.75E-15	2.03E+12	Jankowski et al. (2018)
J1709-1640	25	1640	−1.7	0.07	0.65305	6.31E-15	2.05E+12	Lee et al. (2022)
J1745-3040	88.4	546	−1.7	0.3	0.36743	1.07E-14	2E+12	Malofeev et al. (1994)
J1752-2806	50.4	1100	−2.6	0.16	0.56256	8.13E-15	2.16E+12	Malofeev et al. (1994)
J1820-0427	84	1500	−2.4	0.16	0.59808	6.33E-15	1.97E+12	Malofeev et al. (1994)
J1825-0935	19.4	233	−1.73	0.08	0.76902	5.24E-14	6.42E+12	Izvekova et al. (1981)
J1829-1751	216.8	877	−1.6	0.4	0.30713	5.55E-15	1.32E+12	Malofeev et al. (1994)
J1836-1008	317	756	−2.9	0.39	0.56271	1.18E-14	2.61E+12	Jankowski et al. (2018)
J1844+1454	41.5	3180	−1.9	0.1	0.37546	1.87E-15	8.48E+11	Malofeev et al. (1994)
J1848-0123	159.1	1990	−1.9	0.3	0.65943	5.25E-15	1.88E+12	Malofeev et al. (1994)
J1913-0440	89.4	3220	−2.1	0.16	0.82594	4.07E-15	1.85E+12	Jankowski et al. (2018)
J1921+2153	12.4	15700	−2.41	0.055	1.33730	1.35E-15	1.36E+12	Izvekova et al. (1981)
J1932+1059	3.2	3100	−1.5	0.09	0.22652	1.16E-15	5.18E+11	Lee et al. (2022)
J1935+1616	159	947	−4.7	0.3	0.35874	6.00E-15	1.48E+12	Malofeev et al. (1994)
J1939+2134*	71	235000	−2.59	0.074	0.00156	1.05E-19	4.09E+8	Kuniyoshi et al. (2015)
J1946+1805	16	290000	−3.3	0.1	0.44062	2.41E-17	1.04E+11	Malofeev et al. (1994)
J1948+3540	129.4	1610	−2.4	0.3	0.71731	7.06E-15	2.28E+12	Malofeev et al. (1994)
J2018+2839	14	59700	−2.3	0.15	0.55795	1.48E-16	2.91E+11	Malofeev et al. (1994)
J2022+2854	24.6	2870	−1.67	0.16	0.34340	1.89E-15	8.16E+11	Izvekova et al. (1981)
J2022+5154	22.5	2740	−2.1	0.4	0.52920	3.06E-15	1.29E+12	Malofeev et al. (1994)
J2046+1540	39.8	98900	−1.3	0.4	1.13829	1.82E-16	4.61E+11	Malofeev et al. (1994)

Table 1
(Continued)

Pulsar	DM/pc cm^{-3}	T_c/kyr	α_0	$\nu^0_{\rm peak}$/ GHz	P/s	$P1$	B/G	References
J2048-1616	11.5	2840	−1.1	0.18	1.96157	1.10E-14	4.69E+12	Lee et al. (2022)
J2113+4644	141	22500	−2.3	0.1	1.01468	7.15E-16	8.62E+11	Malofeev et al. (1994)
J2145-0750*	9	8540000	−2.60	0.40	0.01605	2.98E-20	7E+08	Kuniyoshi et al. (2015)
J2149+6329	129.7	35800	−2.0	0.25	0.38014	1.68E-16	2.56E+11	Izvekova et al. (1981)
J2157+4017	71.1	7040	−2.2	0.15	1.52527	3.43E-15	2.32E+12	Malofeev et al. (1994)
J2219+4754	43.5	3090	−2.42	0.065	0.53847	2.77E-15	1.23E+12	Izvekova et al. (1981)
J2225+6535	36	1120	−3.9	0.15	0.68254	9.66E-15	2.6E+12	Malofeev et al. (1994)
J2257+5909	151.1	1010	−2.28	0.20	0.36825	5.75E-15	1.47E+12	Izvekova et al. (1981)
J2305+3100	49.6	8630	−2.3	0.10	1.57589	2.89E-15	2.16E+12	Izvekova et al. (1981)
J2321+6024	94.6	5080	−1.8	0.2	2.25649	7.04E-15	4.03E+12	Malofeev et al. (1994)
J2354+6155	94.7	920	−1.4	0.4	0.94478	1.63E-14	3.97E+12	Malofeev et al. (1994)

We confirmed that 53 pulsars have low-frequency inversion phenomena by investigating the existing literature. In this paper, we carried out a statistical study on these MPS pulsars, investigated their spatial position distribution, the magnetic field-period distribution, peak frequencies, spectral indices, dispersion measures (DMs), and discussed the relationships among these parameters.

2. Fitting Model for MPS Pulsar Spectra

When electrons collide with ions, they not only emit photons and undergo free–free radiation, but they may absorb photons, which causes the free electrons to change from lower kinetic energy free states to higher kinetic energy free states. This process is the inverse of free–free radiation and is known as FFA. Lewandowski et al. (2015) found that the effect of the FFA on the pulsar radiation spectrum is related to the size of the absorption region, the electron density, and the electron temperature. Among them, the FFA is more sensitive to the changes in electron density. Kijak et al. (2017) conducted research on the high-frequency inversion spectra of pulsars using the FFA model, and these high-frequency inverted spectra pulsars are also named gigahertz-peaked spectra (GPS) pulsars. Existing research has shown that the FFA model can describe well the GPS spectra, so in this paper we will also use the FFA model to explain the low-frequency inversion phenomena in MPS pulsars. In this paper, we will adopt the formula given by Swainston et al. (2022) to fit the spectra of pulsar, with its specific form being

$$S_\nu = c\left(\frac{\nu}{\nu_0}\right)^{\alpha} \exp\left[\frac{\alpha}{2.1}\left(\frac{\nu}{\nu_{\rm peak}}\right)^{-2.1}\right], \quad (1)$$

where the reference frequency ν_0 is the geometric mean of the minimum frequency and the maximum frequency, α is the spectral index, $\nu_{\rm peak}$ is the peak frequency, and c is a constant. Here α, $\nu_{\rm peak}$, and c are the parameters to be fitted.

In this paper, we adopt the method proposed by Jankowski et al. (2018) to minimize the different systematic errors introduced by different telescopes when measuring flux densities. In order to minimize the negative impact of these outliers when fitting, this method utilizes the Huber loss function to deal with outliers of the flux density error values, as expressed by

$$R^2 = \sum_i^N \begin{cases} \frac{1}{2}\left(\frac{f_i - y_i}{\sigma_{y,i}}\right)^2 & \text{if } \left|\frac{f_i - y_i}{\sigma_{y,i}}\right| < k \\ k\left|\frac{f_i - y_i}{\sigma_{y,i}}\right| - \frac{1}{2}k^2 & \text{otherwise} \end{cases}, \quad (2)$$

where f_i is the model predictive value, y_i is the actual observation, $\sigma_{y,i}$ is the error value of the flux density, and k defines the distance at which the loss function begins to penalize outliers. In this example, $k = 1.345$ is chosen as the threshold for outliers. According to the proof by Huber (1964), when $\left|\frac{f_i - y_i}{\sigma_{y,i}}\right|$ is less than 1.345, it is considered normal; when $\left|\frac{f_i - y_i}{\sigma_{y,i}}\right|$ is greater than or equal to 1.345, it is considered an outlier. See Swainston et al. (2022) for details on this model-fitting method.

3. Statistical Analysis of MPS Pulsars

We obtained 69 pulsars previously considered to have low-frequency inversion spectra from the literature, as detailed in Table 1, where DM is the dispersion measure, T_c is the characteristic age, P is the period, $P1$ is the period derivative, and B is the pulsar surface magnetic field. These parameters are all from the Australia Telescope National Facility (ATNF) website (Manchester et al. 2005). The spectral index α_0 and peak frequency $\nu^0_{\rm peak}$ are from the references in column 9. Millisecond pulsars in Table 1 are marked with *.

For further inspecting the spectral shape of the pulsars in Table 1, we supplemented the new spectral data provided by the pulsar_spectra software library (Swainston et al. 2022), and further fitted the spectra of these pulsars with Equation (1). According to the new spectral shapes and fitting results, we

Table 2
Pulsars Identified with the Inversion Spectra

Pulsar	α	$\nu_{\rm peak}$/ GHz	χ^2_r
J0034-0721	−2.00	0.05	6.9
J0141+6009	−1.83	0.10	2.4
J0304+1932	−0.75	0.07	7.1
J0323+3944	−2.12	0.07	2.6
J0332+5434	−2.00	0.16	9.8
J0630-2834	−1.40	0.06	14.4
J0809-4753	−2.40	0.13	0.9
J0814+7429	−1.65	0.05	1.5
J0820-1350	−1.65	0.08	13.0
J0826+2637	−1.60	0.06	5.7
J0837+0610	−2.50	0.05	11.8
J0922+0638	−1.90	0.05	10.2
J0943+1631	−1.60	0.06	0.4
J0953+0755	−1.54	0.06	20.3
J1001-5507	−2.36	0.22	1.1
J1012+5307*	−1.70	0.15	4.0
J1057-5226	−2.53	0.19	0.8
J1136+1551	−1.50	0.05	5.8
J1239+2453	−1.27	0.06	2.4
J1509+5531	−2.28	0.07	11.3
J1614+0737	−1.98	0.05	0.7
J1645-0317	−2.50	0.20	17.5
J1752-2806	−2.25	0.13	3.6
J1820-0427	−2.40	0.18	7.3
J1825-0935	−2.20	0.04	18.4
J1829-1751	−1.69	0.20	1.5
J1836-1008	−2.32	0.22	1.5
J1913-0440	−2.80	0.16	3.6
J1921+2153	−2.35	0.06	9.5
J1932+1059	−1.08	0.06	3.4
J1935+1616	−2.10	0.26	5.6
J1946+1805	−1.00	0.06	3.5
J1948+3540	−2.68	0.19	3.5
J2018+2839	−1.57	0.10	7.2
J2022+2854	−1.17	0.06	3.3
J2022+5154	−1.08	0.19	7.4
J2048-1616	−1.49	0.20	5.9
J2113+4644	−1.97	0.17	3.3
J2145-0750*	−2.13	0.17	7.1
J2149+6329	−2.01	0.22	2.1
J2157+4017	−1.82	0.18	9.8
J2257+5909	−2.10	0.18	7.9
J2321+6024	−1.95	0.36	3.7
J2354+6155	−2.00	0.20	6.1

finally found that only 44 pulsars in Table 1 have definite inversion spectra, as shown in Table 2. In Figure 1, we give a fitting of PSR J0809-4753, and other MPS pulsars' fitting results are shown in Appendix A. α and ν_{peak} in Table 2 are newly fitted results according to Equation (1).

Before fitting, we will prejudge the trend of the spectrum. If some data points are far from the trend of the spectrum, these data points may be regarded as outliers. During the fitting, we prioritize ensuring that data points near 1 GHz conform to the power-law spectral model because the spectral turn-up or

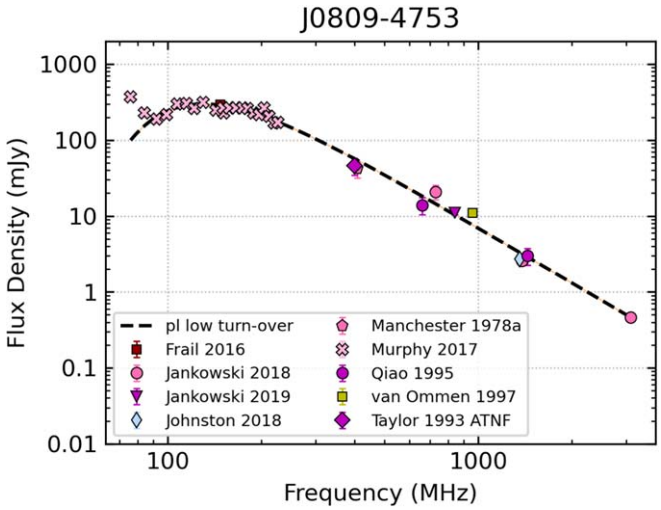

Figure 1. The fitting spectrum of J0809-4753 by the FFA model.

flattening phenomena in general appear in the higher-frequency bands (Maron et al. 2000). When fitting, we will also prioritize adopting the data points from the interferometric imaging observations which are less affected by scattering. For example, there are interferometric imaging observations from Murphy et al. (2017) for PSR J0820-1350, and we will prioritize guaranteeing the fitting of these data. But in some cases, it is difficult to judge which points are outliers, especially at low frequencies, due to the scarce data coverage. For example, it is difficult to judge which point is the outlier near 100 MHz for PSR J2354+1655. This situation can only rely on future observations.

The spectral parameters in Table 2 may differ from those in Table 1 due to introducing the latest data when fitting. During investigating the literature of MPS pulsars, we also found nine pulsars with spectral breaks that actually have the characteristics of inversion spectra, so these pulsars were also fitted using the FFA model, and the fitting results are shown in Table 3 and Figure 2, with α_0 from the references in Table 3. These pulsars were categorized as spectrally broken pulsars by Bilous et al. (2016) and Murphy et al. (2017).

Based on the statistical results in Tables 2 and 3, we obtained 53 MPS pulsars in total. In the following section, we will carry out a statistical analysis on these MPS pulsars.

3.1. MPS Pulsars Spatial Distribution

We show the spatial distribution of the 53 MPS pulsars in the Galactic coordinate system in Figure 3. It can be seen from Figure 3 that most of the MPS pulsars are mainly distributed in the low Galactic latitude region. Figure 4 displays the projected distribution of these pulsars on the Galactic plane, where the horizontal and vertical coordinates are the Galactic plane coordinate components XX and YY, respectively, the

Table 3
MPS Pulsars Were Thought to Have Spectral Breaks in the Past

Pulsar	DM/pc cm^{-3}	T_c/kyr	α_0	α	$\nu_{\rm peak}$/ GHz	χ_r^2	P/s	$P1$	B/G	References
J0946+0951	15.3	4980	−2.60	−2.60	0.04	1.8	1.09771	3.49E-15	1.98E+12	Bilous et al. (2016)
J1115+5030	9.2	10500	−2.20	−1.52	0.05	6.9	1.65644	2.49E-15	2.06E+12	Bilous et al. (2016)
J1321+8323	13.3	18700	−2.50	−0.69	0.06	0.5	0.67004	5.66E-16	6.23E+11	Bilous et al. (2016)
J1532+2745	14.7	22900	−1.60	−1.64	0.05	0.6	1.12484	7.80E-16	9.48E+11	Bilous et al. (2016)
J1543-0620	18.0	12800	−1.70	−1.70	0.07	5.0	0.70906	8.80E-16	7.99E+11	Murphy et al. (2017)
J1635+2418	24.3	65100	−2.30	−1.79	0.05	0.9	0.49051	1.19E-16	2.45E+11	Bilous et al. (2016)
J1741+2758	29.1	11700	−2.00	−1.70	0.05	0.7	1.36074	1.84E-15	1.6E+12	Bilous et al. (2016)
J1840+5640	26.8	17500	−1.60	−1.49	0.05	1.5	1.65286	1.49E-15	1.59E+12	Bilous et al. (2016)
J1907+4002	31.0	36200	−2.10	−1.96	0.18	1.1	1.23576	5.41E-16	8.27E+11	Bilous et al. (2016)

Note. DM, T_c, P, $P1$, and B are all from the ATNF website. α_0 is from the references in the last column, and α, $\nu_{\rm peak}$, and χ_r^2 are the new fitting results according to the new spectral data from the pulsar_spectra software library (Swainston et al. 2022).

coordinates of the Galactic center are (0, 0) and the coordinates of the Sun are (0, 8.5 kpc) (Kerr & Lynden-Bell 1986).

We depict the statistical distribution of the distances of 53 MPS pulsars from the Galactic center in Figure 5. It can be seen from Figure 5 that most MPS pulsars tend to be distributed on one side of the solar system like other normal radio pulsars (Xu et al. 2011), and the mean distance of these sources from the Galactic center is 8.31 kpc. The distribution is also characterized by a Gaussian distribution, whose peak is around 8.74 kpc. This phenomenon may be due to observational selection effects (including interstellar dispersion and scattering) (Xu et al. 2011).

3.2. B–P *Distribution of MPS Pulsars*

Using data from the ATNF Pulsar Catalogue (Manchester et al. 2005), we plotted the magnetic field–period (B–P) distributions of the 53 MPS pulsars in Figure 6. Except for two millisecond pulsars, 51 MPS pulsars have an average magnetic field strength of 1.75×10^{12} Gs and an average rotation period of 0.95 s.

It can be seen from Figure 6 that five MPS pulsars (including two millisecond pulsars) are located between the spin-up line (Bhattacharya & van den Heuvel 1991) and the death line (Taylor & Stinebring 1986). These five pulsars have an average DM of 12 pc cm^{-3}, and the remaining 48 MPS pulsars have an average DM of 57 pc cm^{-3}. This suggests that the MPS pulsars located between the spin-up and the death line are likely to have a lower DM than the other MPS pulsars.

3.3. *Peak Frequency Statistics of MPS Pulsars*

The peak frequency distribution of the 53 MPS pulsars is shown in Figure 7. The average peak frequency of the 53 MPS pulsars is 0.12 GHz. It can be seen from Figure 7 that the peak frequencies of the 48 MPS pulsars are mainly distributed below 0.20 GHz, which accounts for 91% of the total number of MPS pulsars.

We further performed a statistical analysis of the correlation between the peak frequencies of the MPS pulsars and other parameters. Statistical analysis shows that the peak frequency $\nu_{\rm peak}$ of the MPS pulsar is weakly correlated with the characteristic age T_c, with a Pearson correlation coefficient of −0.19. In addition, Izvekova et al. (1981) suggested that there is a correlation between $\nu_{\rm peak}$ and period P for MPS pulsars, but we do not find a significant correlation between $\nu_{\rm peak}$ and P for the MPS pulsars sample in this paper. The correlation between $\nu_{\rm peak}$ and P needs further observations to check.

3.4. *Spectral Index Distribution of MPS Pulsars*

Figure 8 shows the spectral index distribution of MPS pulsars, with an average spectral index of −1.85. J1913-0440 has the steepest spectral index, −2.80, and J1321+8323 has the flattest spectral index, −0.69, in the MPS pulsars sample. In addition, we obtained J1614+0737 with a spectral index of −1.98, which is flatter than the spectral index of −3.80 determined by Malofeev et al. (1994), and this difference in spectral indices may be due to the small number of available data points in Malofeev et al. (1994).

According to Tables 1 and 3, the average value of the spectral index of the 53 MPS pulsars given by the previous authors is −2.23. In this paper due to the addition of new spectral data, the average value of the spectral index obtained by fitting with the FFA model is −1.85, which is flatter than the previous results. Jankowski et al. (2018) suggested that the gradual flattening of the spectral indices of the pulsars may be a trend, and that this trend may be strengthened with further observations at both low and high frequencies.

We also investigated the correlation between the distance $|z|$ of the MPS pulsar from the Galactic plane and its spectral index, and did not find a significant correlation between $|z|$ of the MPS pulsar and its spectral index.

3.5. *DM Distribution*

The DM distribution of the 53 MPS pulsars is shown in Figure 9, with a mean DM dispersion of 53 pc cm^{-3}. From

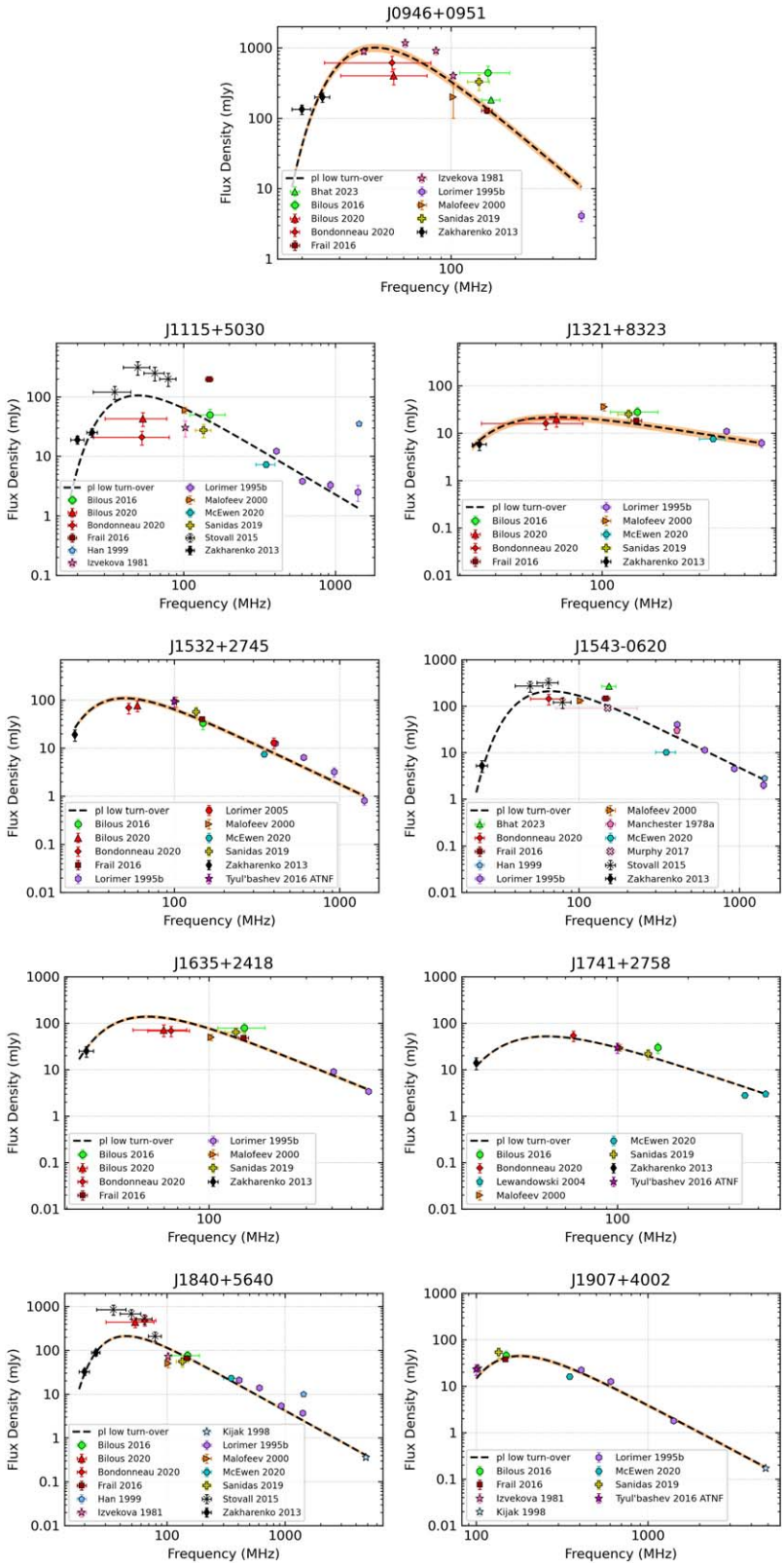

Figure 2. MPS pulsars thought to have broken power law spectral shapes.

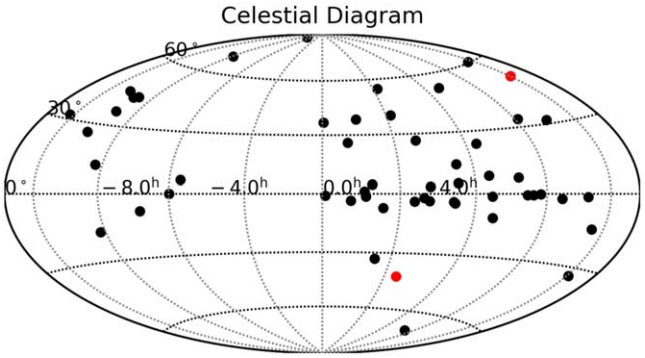

Figure 3. Spatial distribution of MPS pulsars in the Galactic coordinate system. The red dots represent millisecond pulsars.

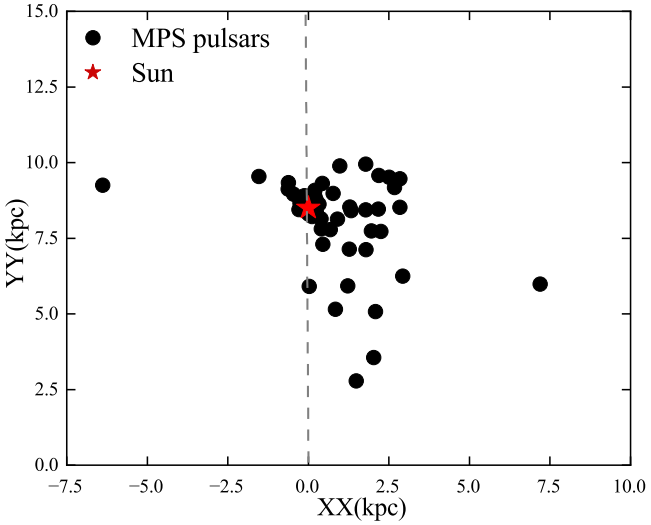

Figure 4. Projected distribution of MPS pulsars on the Galactic plane.

Figure 9, we can see that 38 MPS pulsars have a dispersion distribution between 0 and 50 pc cm^{-3}, accounting for 72% of the total. As a comparison, we also calculated the average DM of 3267 pulsars in the ATNF Pulsar Catalogue (Manchester et al. 2005); its average DM is 204 pc cm^{-3} and is much higher than the one of MPS pulsars. The lower average DM of the MPS pulsars compared to the one from the ATNF Pulsar Catalogue is obviously due to the selection effect of the MPS pulsar sample, i.e., many of the pulsars with higher DMs are fully scattered at low frequencies, and therefore no flux density measurements are available.

4. Discussion

By fitting and analyzing the available spectral data, we have identified that 44 pulsars in Table 1 have low-frequency inversions. Although the remaining 25 pulsars in Table 1 were once thought to have low-frequency inversions, these 25

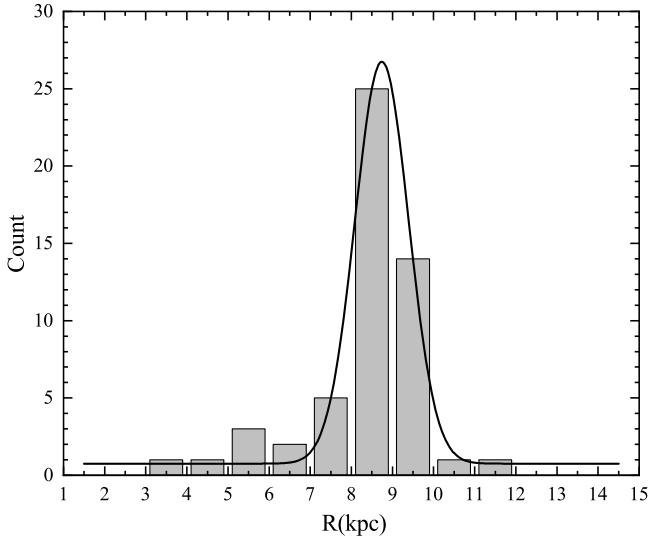

Figure 5. Statistical distribution of the distances of MPS pulsars from the Galactic center, where the curve represents the Gaussian fitting.

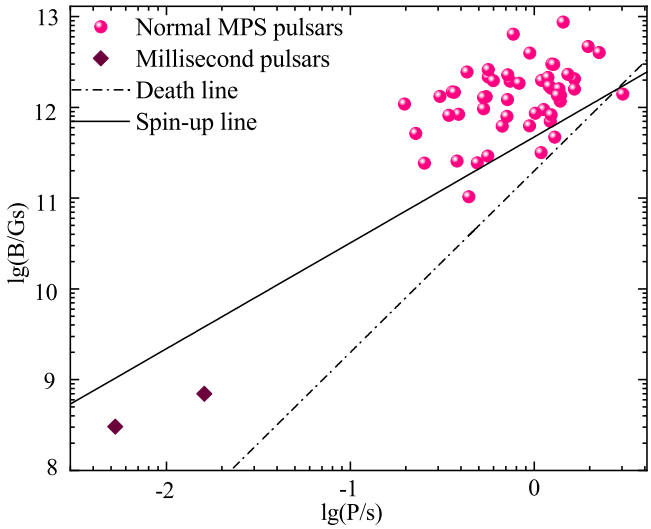

Figure 6. Magnetic field–period (B–P) distribution of MPS pulsars.

pulsars do not exhibit significant inversion phenomena based on the newly published spectral observation data. We give the fitting results of these 25 pulsars in Appendix B with the power-law model.

For comparison with the MPS pulsars, we also statistically analyzed the parameters of all pulsars from the ATNF Pulsar Catalogue (Manchester et al. 2005). The average age of MPS pulsars is 2.8×10^5 kyr, which is less than the one in the ATNF Pulsar Catalogue, 1.7×10^6 kyr. The average period derivative of MPS pulsars is 5.22×10^{-15} s $\cdot$ s^{-1}, which is smaller than the one in the ATNF Pulsar Catalogue, 4.03×10^{-13} s $\cdot$ s^{-1}. In

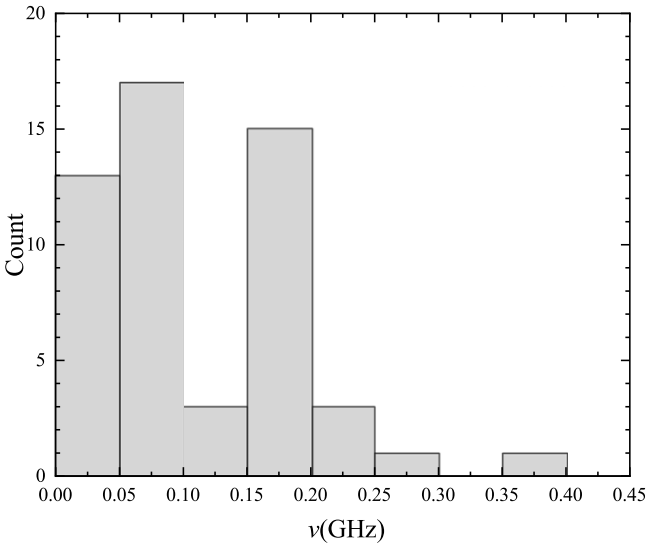

Figure 7. Peak frequency distribution of MPS pulsars.

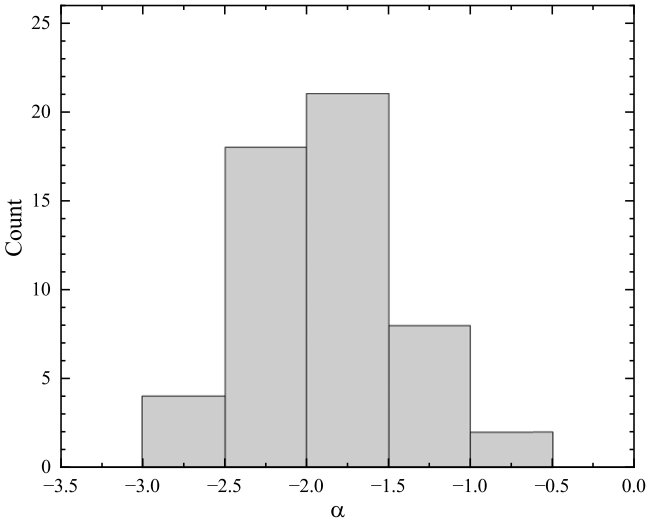

Figure 8. Spectral index distribution of MPS pulsars.

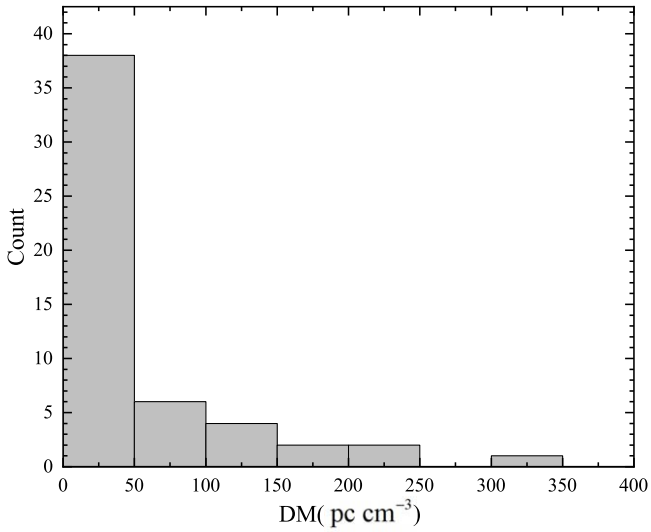

Figure 9. DM distribution of MPS pulsars.

addition, the mean value of the MPS pulsar distance (from the Earth to the pulsar) is 1.86 kpc, which is much smaller than the one in ATNF Pulsar Catalogue, 6.04 kpc. We think that the smaller distance of MPS pulsars may be due to the observation selection effect. The identification of spectral inversion relies heavily on the low-frequency observations, but the low-frequency observations of pulsars are seriously affected by the dispersion and scattering, so only nearby pulsars have the low-frequency data and can be identified as MPS pulsars.

Lorimer et al. (1995) studied 343 pulsars and explored the correlations between the spectral indices α, and parameters such as P, $P1$, T_c, B, and the rate of rotational energy loss $\dot{E}$. They found the correlation between the spectral index and the characteristic age is relatively strong. Maron et al. (2000) studied 281 pulsars and did not find any significant correlations between the spectral indices and the periods, the period derivatives, the characteristic ages, or other parameters. So, we also analyzed the correlations between the spectral indices of MPS pulsars and other parameters, and the results show that there are no significant correlations between their spectral indices and periods, period derivatives, or characteristic ages. On the other hand, we found that DM has a relatively strong correlation with the spectral index, with a correlation coefficient of -0.47, as shown in Figure 10, but this correlation may be an observational selection effect. The greater DM means that a stronger radio emission at a low frequency is needed when observing, so MPS pulsars have a the steeper spectral index. We further explore the correlations of MPS pulsars' DMs with their peak frequencies and ages (see Figure 10), and the corresponding correlation coefficients are 0.67 and -0.45, respectively. The strong correlation between MPS pulsars' DMs and their peak frequencies indicates the low-frequency inversion is related to the interstellar medium, and further indicates that the FFA from the interstellar medium may be the cause of the low-frequency inversion. The correlation between MPS pulsars' DMs and their ages suggests that the interstellar medium is an important factor influencing the evolution of MPS pulsars.

To further understand the nature of MPS pulsars, we compared MPS pulsars with GPS pulsars. Kijak et al. (2021) listed 33 GPS pulsars discovered so far. The GPS pulsars are generally young, 27 of 33 GPS pulsars have an age of less than 10^3 kyr, whereas the MPS pulsars are older, with an average age of 2.8×10^5 kyr; the mean spectral index of the MPS

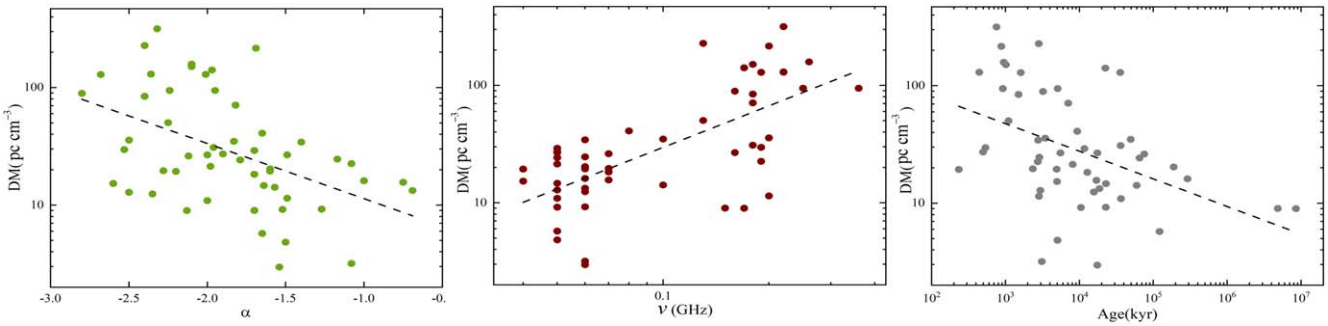

Figure 10. The correlations of MPS pulsars' DMs with spectral indices, peak frequencies, and ages, from left to right respectively.

pulsars is −1.85, whereas the GPS pulsars are flatter than the MPS pulsars, with a mean spectral index of −1.46; and the average DM of the MPS pulsars is 53 pc cm^{-3}, whereas the mean DM of the GPS pulsars is as high as 346 pc cm^{-3}, i.e., the mean DM of the MPS pulsars is much smaller than the one for GPS pulsars.

We further explored the GPS pulsars' correlation coefficients between DMs and the spectral indices, peak frequencies, and ages, and the corresponding correlation coefficients are −0.05, 0.50, and −0.35, respectively. The corresponding correlation coefficients of MPS pulsars are −0.47, 0.67, and −0.45, respectively, which make it appear that DM has a more significant effect on MPS pulsars.

The low-frequency data are important for judging the turn-over characteristic of a pulsar's spectrum, but the low-frequency data are vulnerable to scattering. So, in order to estimate the effect of the scattering on the MPS pulsars' data at the lowest frequencies, we calculated the pulse-broadening times τ_d according to Bhat et al. (2004), and then obtained the ratio of the pulse-broadening time to the pulsar's period $\frac{\tau_d}{P}$. We found that only four pulsars, J1836-1008, J1829-1751, J0809-4753, and J2257+5909, have such ratios that are larger than 1 at the lowest frequencies in their spectra, which are 12.01, 2.9, 2.15, and 1.64, respectively. Although the first three pulsars J1836-1008, J1829-1751, and J0809-4753 have large $\frac{\tau_d}{P}$ ratios, i.e., the pulse smearing effects from scattering are large, their spectral data at the lowest frequencies adopted in this paper were from the interferometric imaging observations, which are less effected by the scattering. PSR J2257+5909 has the $\frac{\tau_d}{P}$ value 1.64 at 102 MHz, and the flux density at 102 MHz was measured by the pulse profile measurements, which may have large error due to the scattering. So overall, the low-frequency data of 53 MPS pulsars except for PSR J2257+5909 are less effected by the scattering. The turn-over characteristic of PSR J2257+5909 needs further confirmation by future low-frequency observations.

5. Conclusion

We identified 53 pulsars with low-frequency inversion characteristics by fitting and analyzing the available pulsar multi-band data. The spatial positions, *B*–*P* distribution, peak frequencies, spectral indices, and DM of these 53 MPS pulsars were statistically studied. Compared with the corresponding average values of pulsars in the ATNF Pulsar Catalogue, the average characteristic age, the average DM, and the average distance to the Earth of MPS pulsars are all smaller. We find a strong correlation between the spectral indices and DMs, indicating that DM may be an important factor affecting the spectral indices of MPS pulsars. We also find a strong positive correlation between DMs and the peak frequencies, and negative correlation between DMs and the ages of MPS pulsars. These results suggest that the interstellar medium is an important cause to form this low-frequency inversion spectrum, and further demonstrate that the FFA is an important mechanism for low-frequency inversion of pulsars. It is obvious that this sample is biased to the pulsars with small DMs because the identification of an MPS pulsar mainly relies on low-frequency observations, and pulsars with smaller DMs are easier to observe. So, more low-frequency observations and larger MPS pulsar sample sets are needed to confirm these statistical results.

Acknowledgments

This work was supported in part by Chunhui plan international cooperation project of China Education Ministry under grants 202201406 and HZKY20220171.

Appendix A
The Fitting Spectra of 44 Identified MPS Pulsars in Table 1

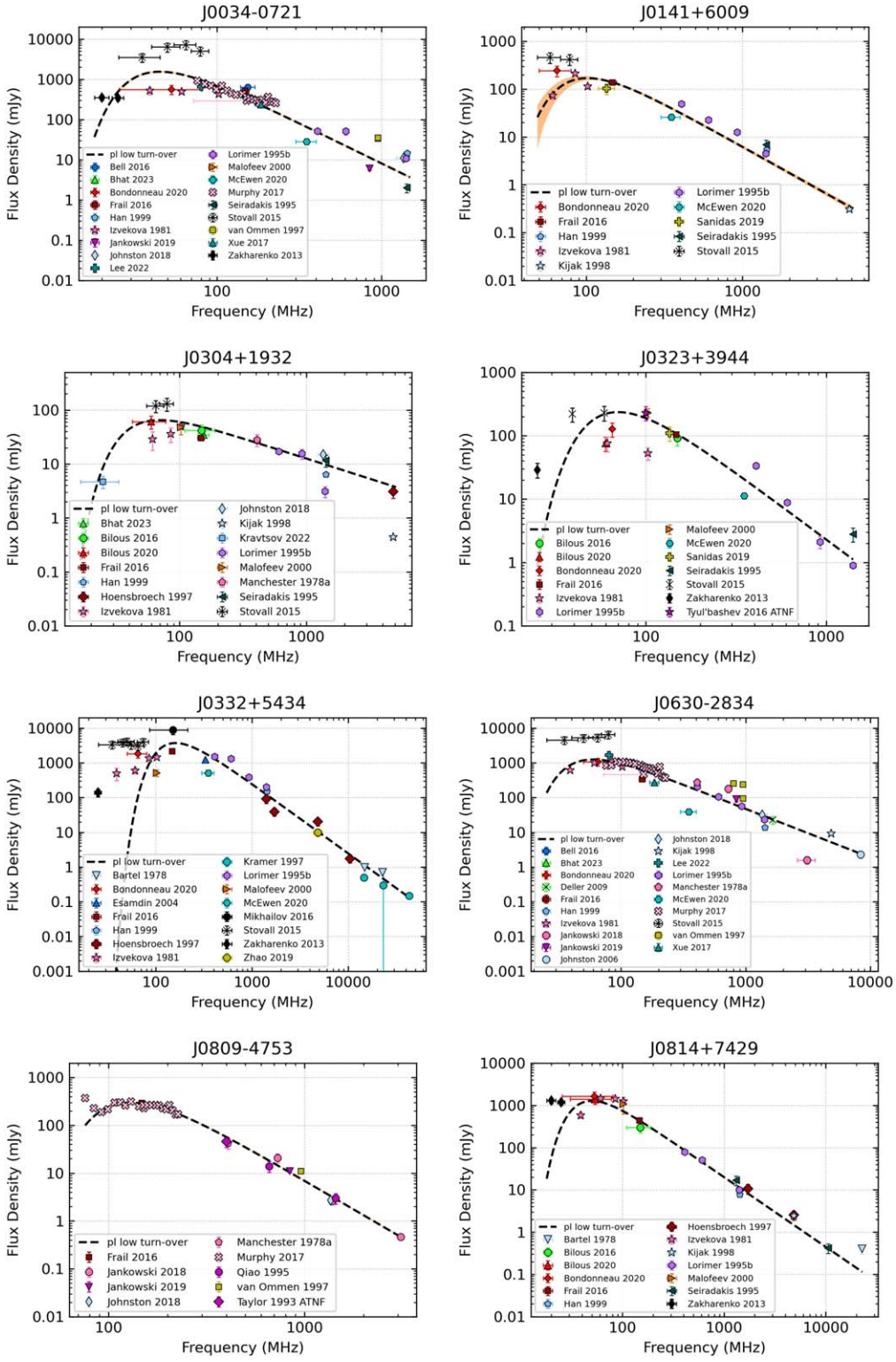

Figure A1. The spectra of 44 identified MPS pulsars in Table 1. The curves represent the fitting by the FFA model.

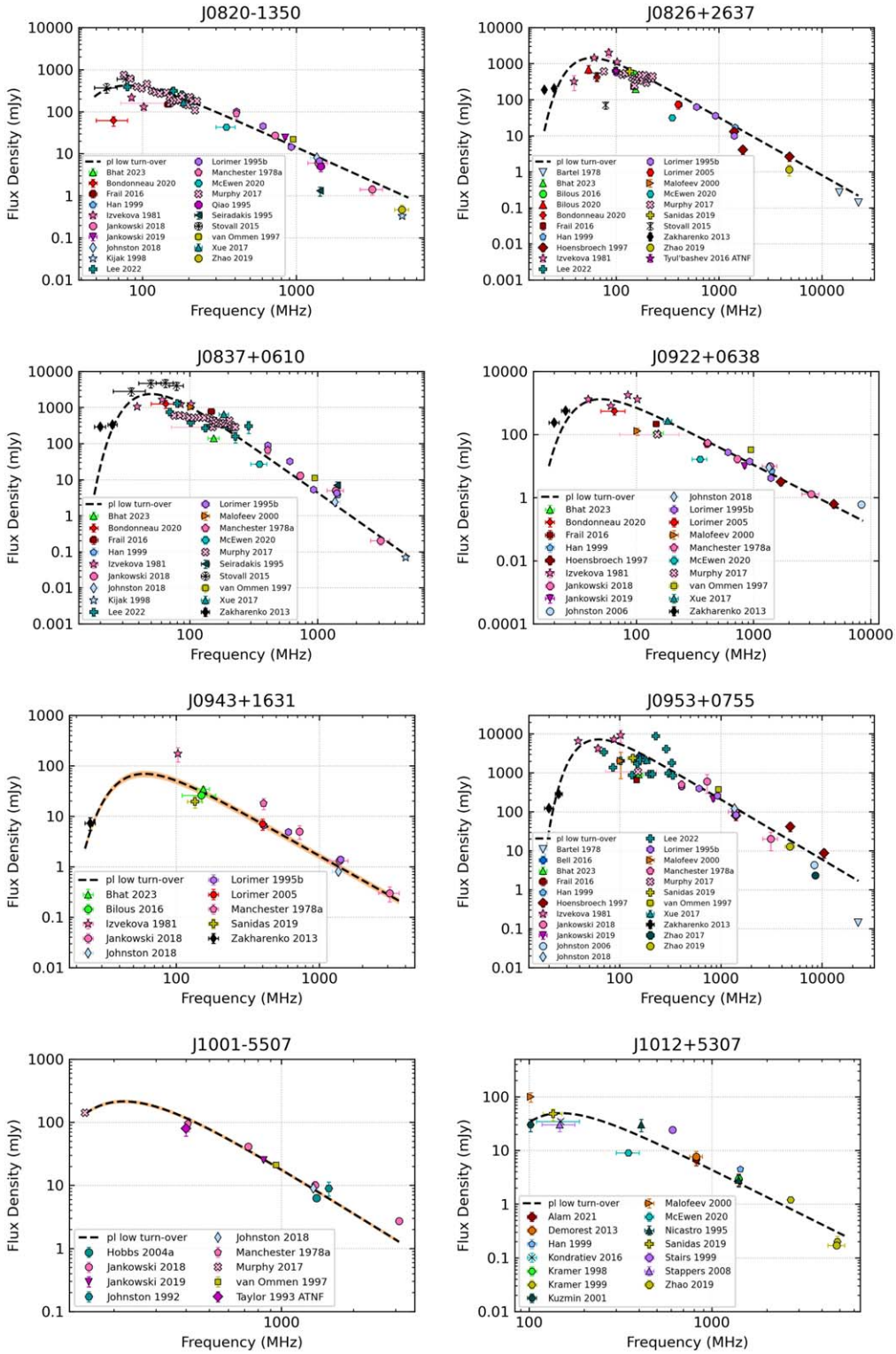

Figure A1. (Continued.)

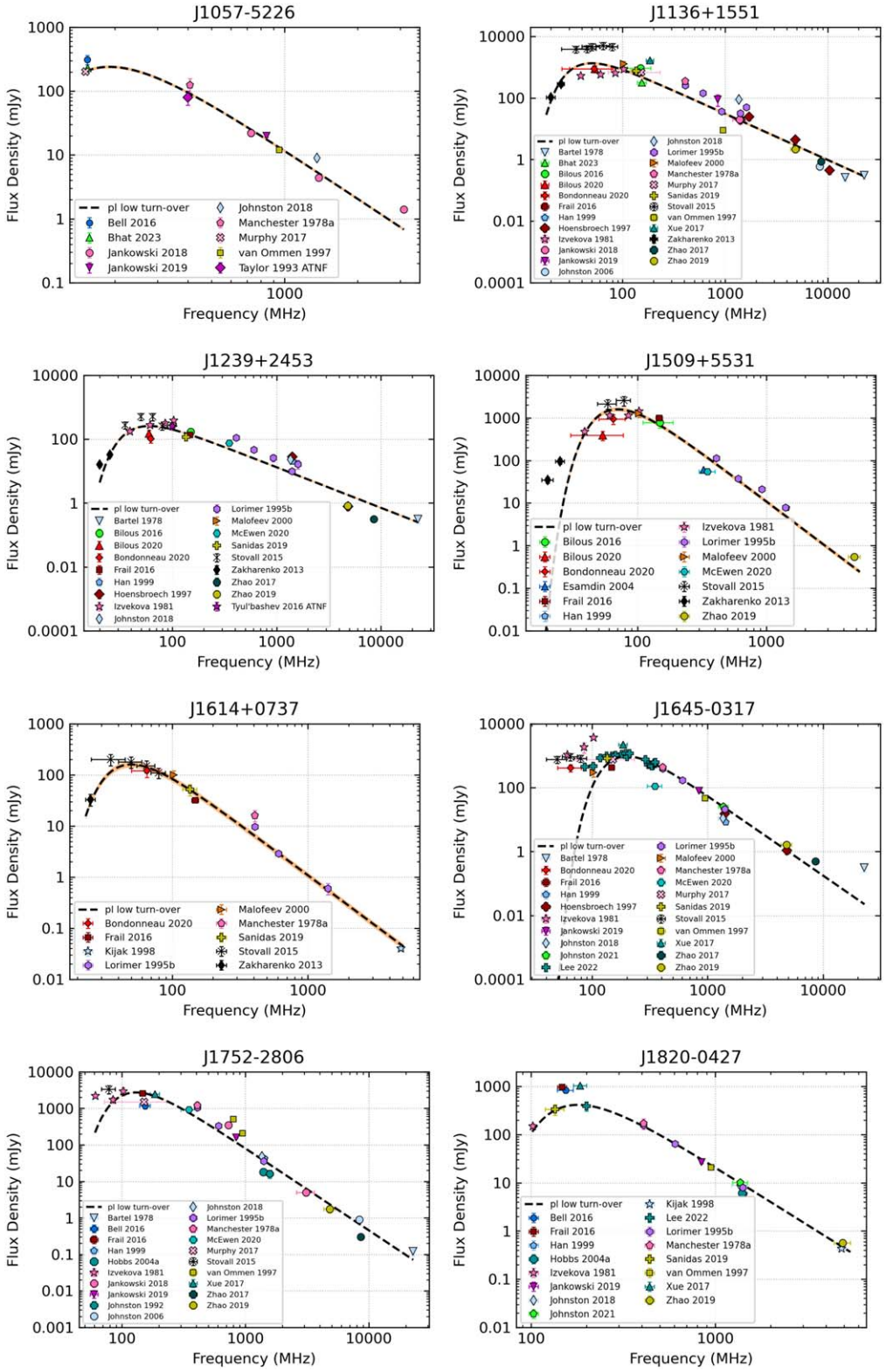

Figure A1. (Continued.)

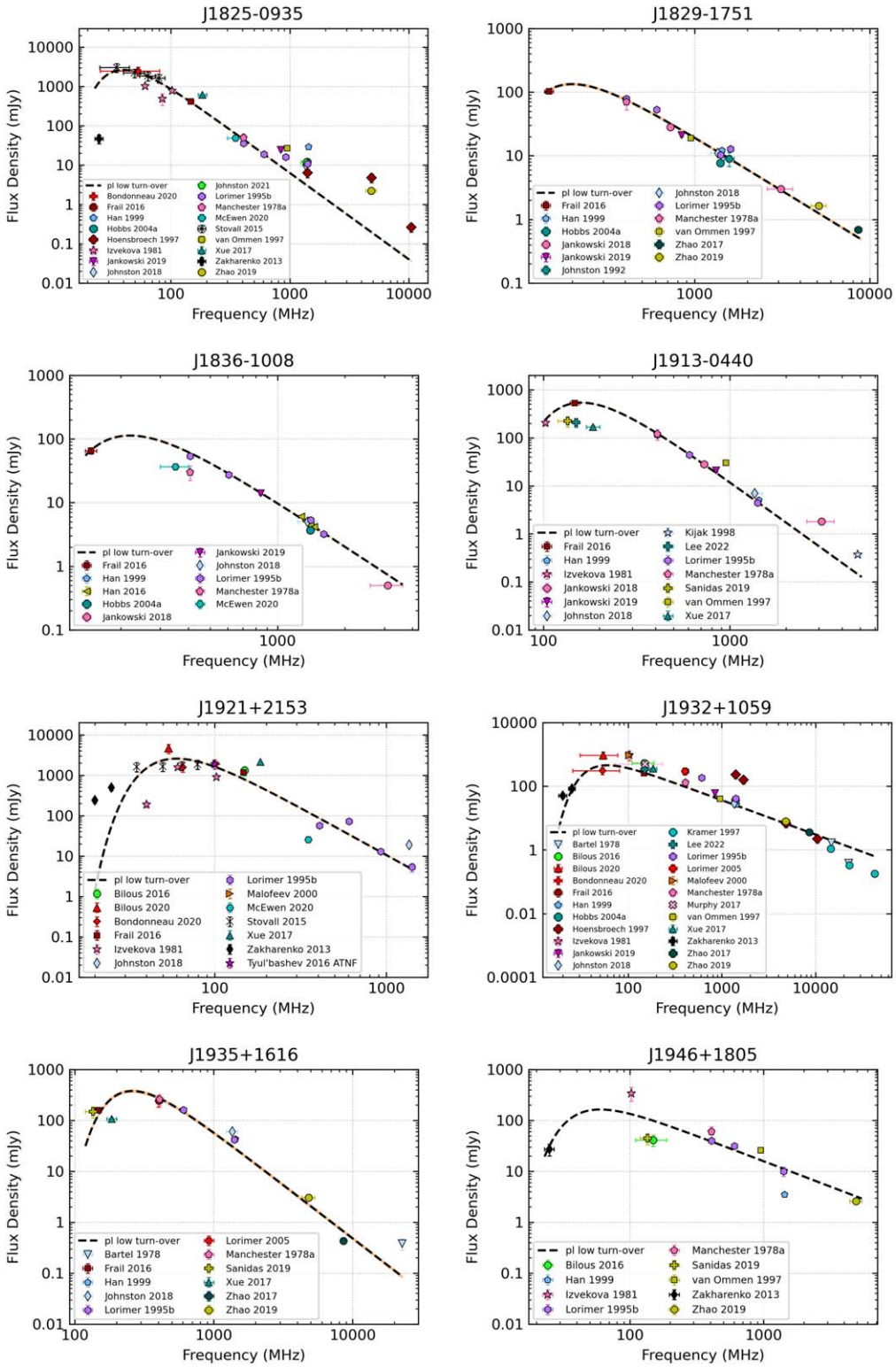

Figure A1. (Continued.)

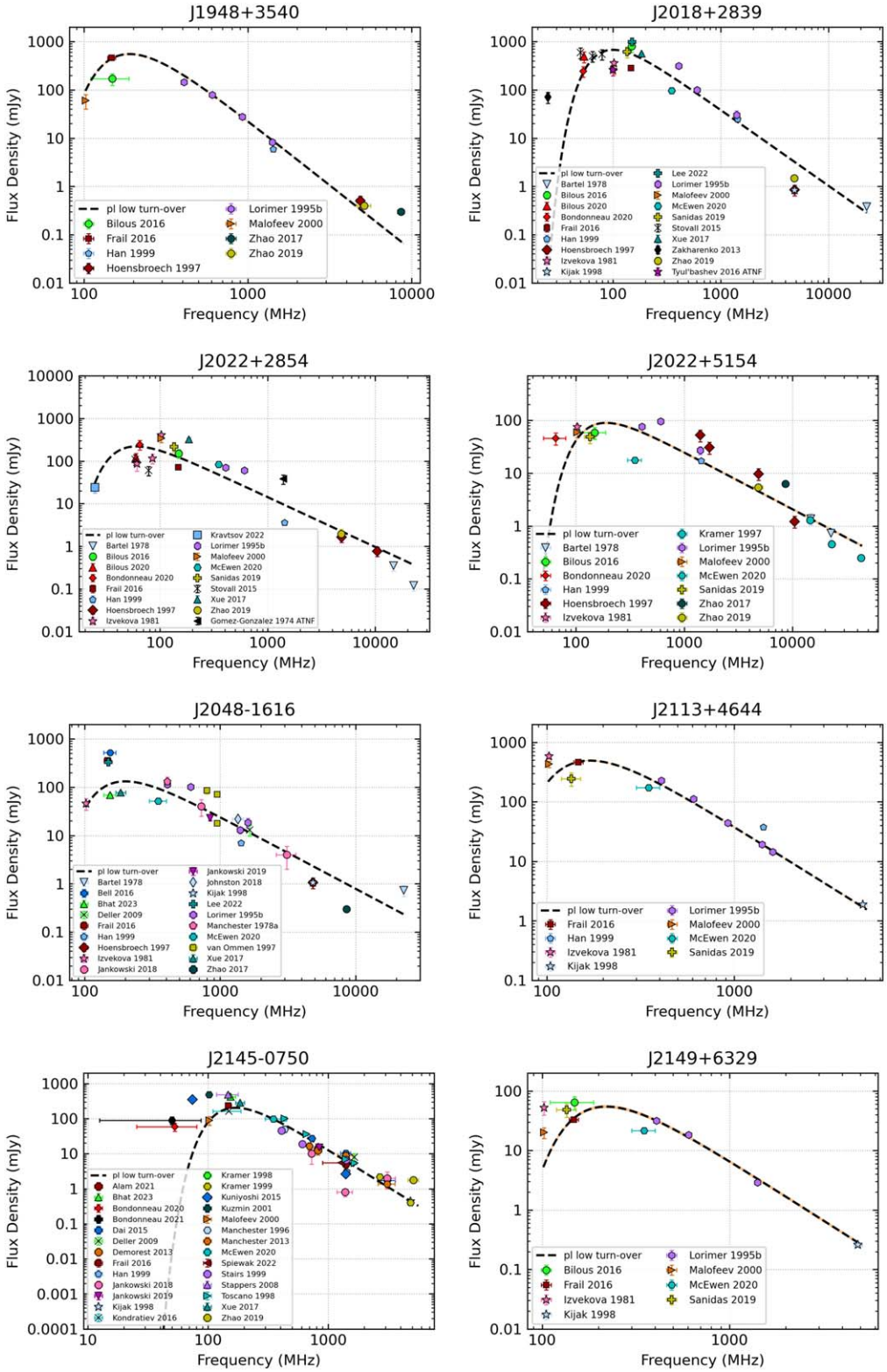

Figure A1. (Continued.)

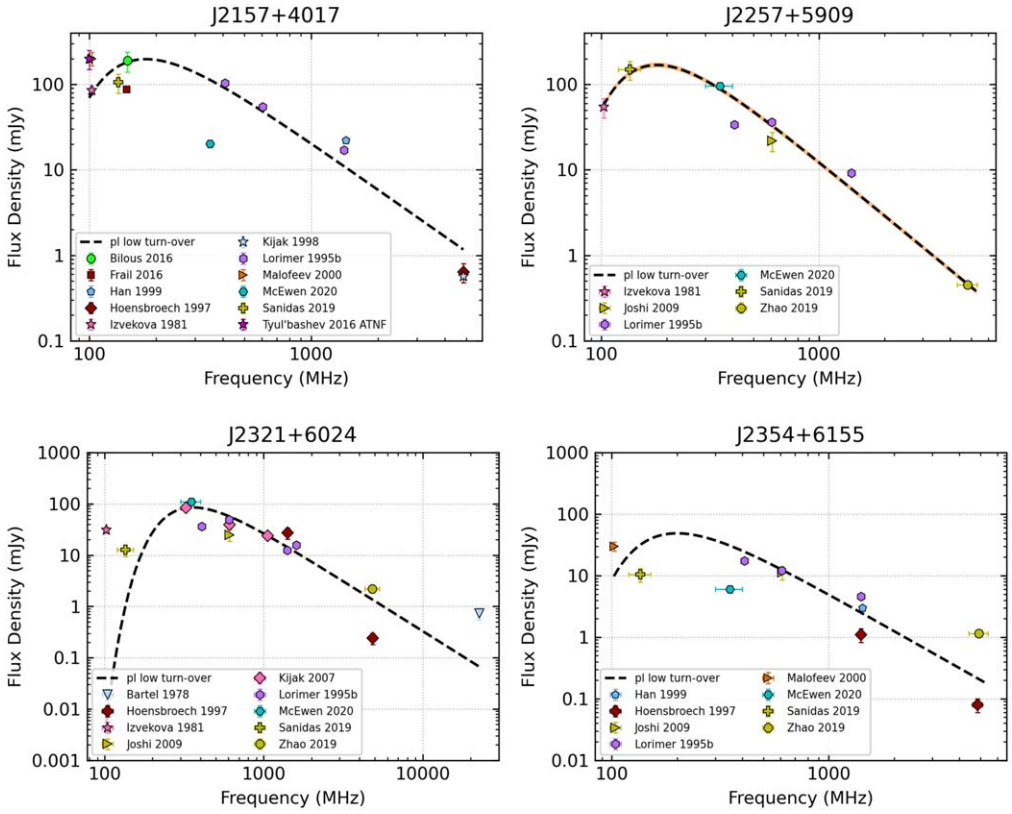

Figure A1. (Continued.)

Appendix B
The Spectra of 25 Pulsars in Table 1 Without the Inversion Phenomena

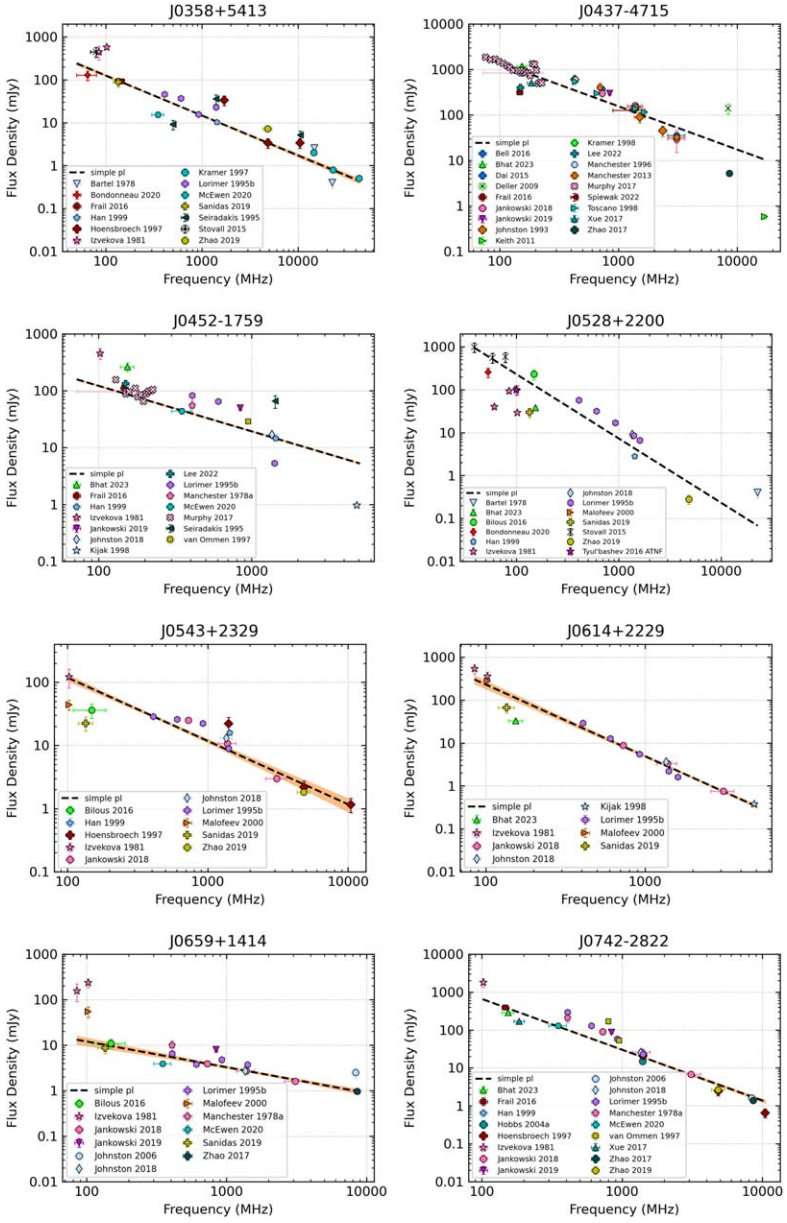

Figure B1. 25 pulsars in Table 1 without the inversion phenomena. The curves represent the power-law model.

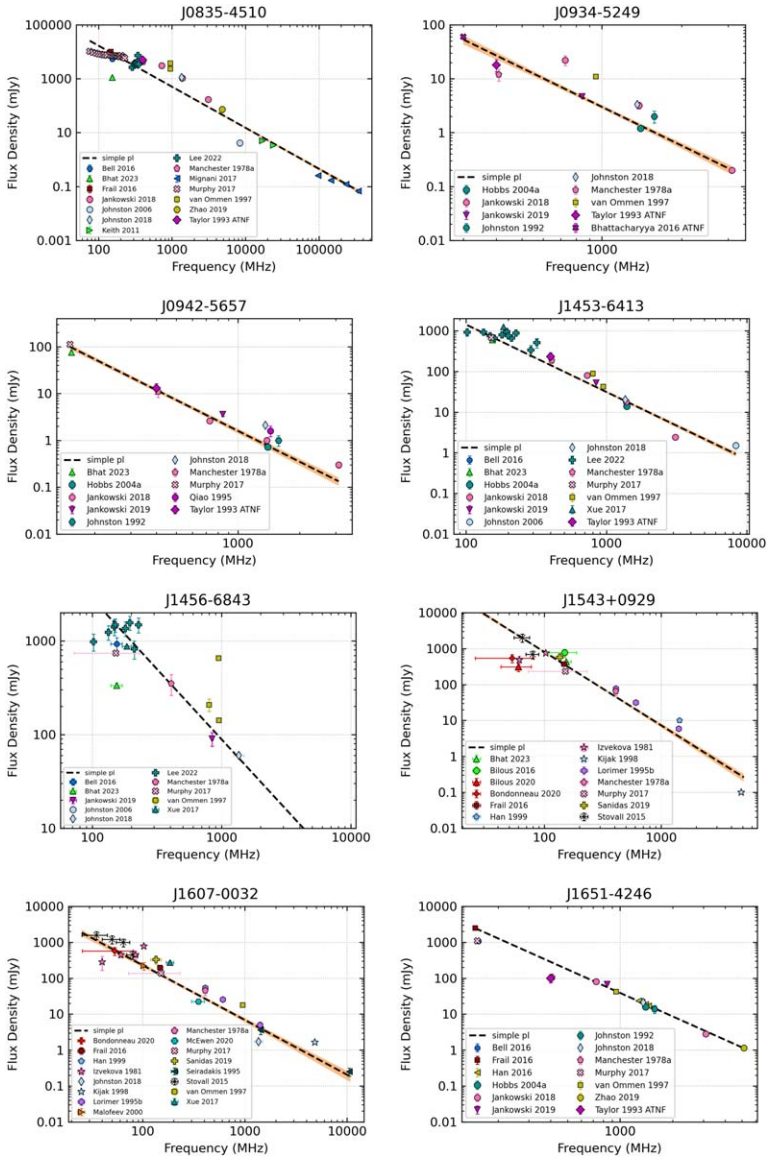

Figure B1. (Continued.)

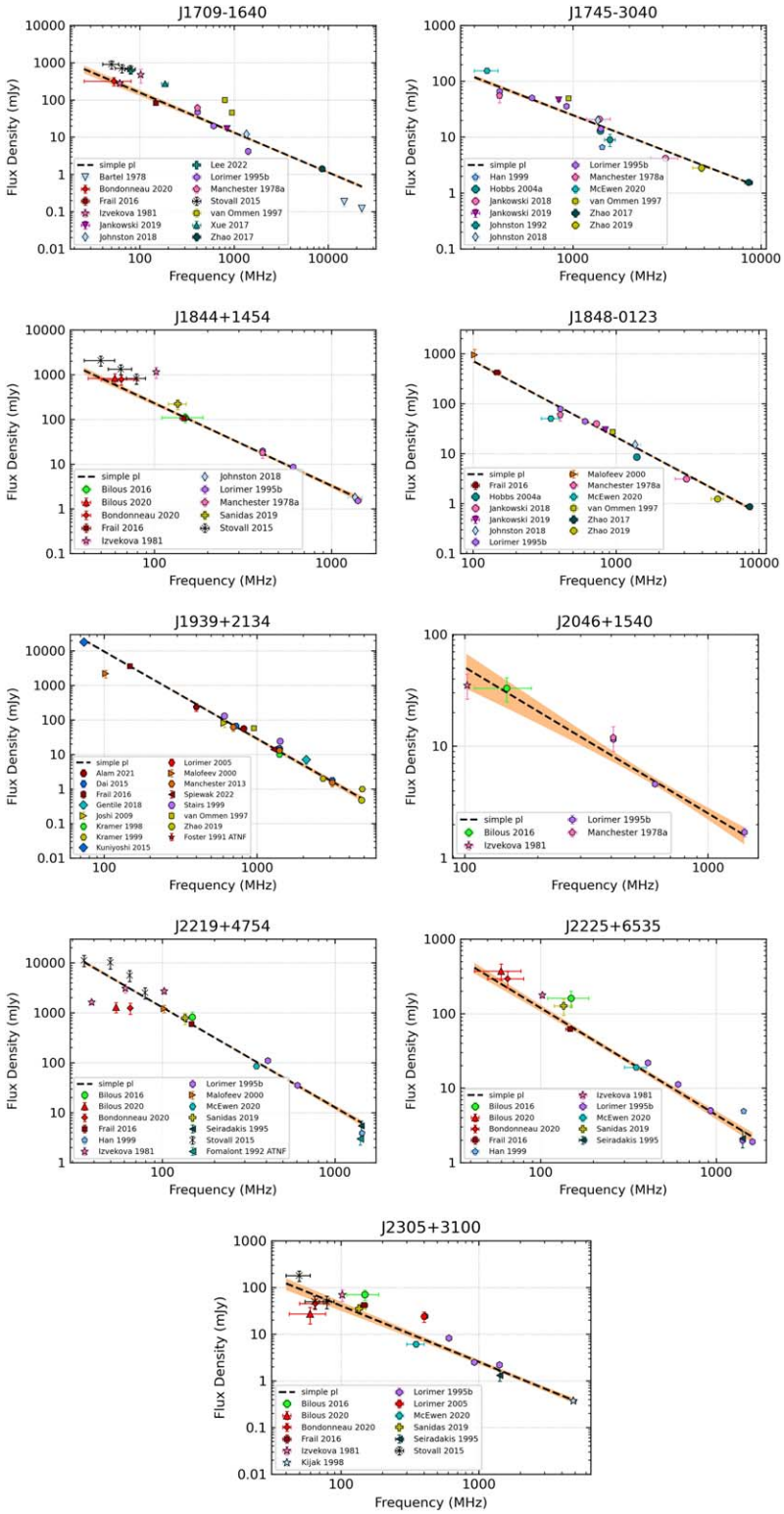

Figure B1. (Continued.)

References

Bhat, N. D. R., Cordes, J. M., Camilo, F., Nice, D. J., & Lorimer, D. R. 2004, ApJ, 605, 759
Bhattacharya, D., & van den Heuvel, E. P. J. 1991, PhR, 203, 1
Bilous, A. V., Kondratiev, V. I., Kramer, M., Keane, E. F., et al. 2016, A&A, 591, A134
Cong, Y., Yue, B., Xu, Y., et al. 2021, ApJ, 914, 128
Huber, P. J. 1964, Ann. Math. Statist., 35, 73
Izvekova, V. A., Kuzmin, A. D., Malofeev, V. M., & Shitov, I. P. 1981, Ap&SS, 78, 45
Jankowski, F., van Straten, W., Keane, E. F., et al. 2018, MNRAS, 473, 4436
Kellermann, K. I. 1966, AuJPh, 19, 195
Kerr, F. J., & Lynden-Bell, D. 1986, MNRAS, 221, 1023
Kijak, J., Basu, R., Lewandowski, W., & Rożko, K. 2021, ApJ, 923, 211
Kijak, J., Basu, R., Lewandowski, W., Rożko, K., & Dembska, M. 2017, ApJ, 840, 108
Kuniyoshi, M., Verbiest, J. P. W., Lee, K. J., et al. 2015, MNRAS, 453, 828
Kuzmin, A. D., & Losovsky, B. Y. 2001, A&A, 368, 230
Lee, C. P., Bhat, N. D. R., Sokolowski, M., et al. 2022, PASA, 39, e042
Lewandowski, W., Rożko, K., Kijak, J., & Melikidze, G. I. 2015, ApJ, 808, 18
Lorimer, D. R., Yates, J. A., Lyne, A. G., & Gould, D. M. 1995, MNRAS, 273, 411
Malofeev, V. M., Gil, J. A., Jessner, A., et al. 1994, A&A, 285, 201
Manchester, R. N., Hobbs, G. B., Teoh, A., & Hobbs, M. 2005, AJ, 129, 1993
Marcote, B., Ribó, M., Paredes, J. M., & Ishwara-Chandra, C. H. 2015, MNRAS, 451, 59
Maron, O., Kijak, J., Kramer, M., & Wielebinski, R. 2000, A&AS, 147, 195
Murphy, T., Kaplan, D. L., Bell, M. E., et al. 2017, PASA, 34, e020
Sieber, W. 1973, A&A, 28, 237
Swainston, N. A., Lee, C. P., McSweeney, S. J., & Bhat, N. D. R. 2022, PASA, 39, e056
Taylor, J. H., & Stinebring, D. R. 1986, ARA&A, 24, 285
Wang, P., Li, D., Clark, C. J., et al. 2021, SCPMA, 64, 129562
Xu, X., Wang, C., Han, J., & Hu, L. 2011, SCPMA, 54, 552
Zhang, C. M., & Kojima, Y. 2006, MNRAS, 366, 137